Detecting Gamma-ray Pulsations from Radio Pulsars

ARCC Scholar thesis For Graduation

in partial fulfillment of the requirements
of the ARCC Scholar program

S. Cohen

May 3, 2013

Abstract

Using data from the *Fermi* LAT survey, we evaluate ten known newly discovered radio pulsars, following standard analysis procedures, to see if detection of gamma-ray pulsations from these pulsars can be made. Given the number of radio pulsars discovered from gamma-ray point sources in the *Fermi* LAT survey, we hope to find gamma-ray pulsars among these ten pulsars. In order to demonstrate our capability of detecting gamma-ray emission, we first confirm detection of gamma-ray pulsations for the known radio and gamma-ray pulsar J1816+4510. The H-test, along with its corresponding false alarm probability, is the statistical test by which we identify whether or not significant gamma-ray pulsations have been detected. For the ten pulsars other than J1816+4510, our H statistic value was not large enough to claim detection of gamma-ray pulsations.

Glossary of Abbreviations and Symbols

GLAST	Gamma-ray Large Area Space Telescope
LAT	Large Area Telescope
EGRET	Energetic Gamma Ray Experiment Telescope
PSR	Pulsar
MSP	Millisecond Pulsar
PSC	Pulsar Search Consortium
RA	Right Ascension
DEC	Declination
MJD	Modified Julian Date

Contents

1 Introduction

The *Fermi* Gamma Ray Space Telescope, formerly known as the Gamma Ray Large Area Space Telescope (GLAST), is an international, multi-agency space observatory which collects high-energy data [1]. The principle scientific instrument of the *Fermi* spacecraft is the Large Area Telescope (LAT).

Fermi has identified 35 gamma-ray pulsars from blind frequency searches of the LAT survey. The survey consists of all gamma-ray data taken from the entire sky since the date of *Fermi's* first mission. A total of 43 new millisecond radio pulsars were found in searches of *Fermi* point sources without associations to known gamma-ray emitting source classes [2]. The Energetic Gamma Ray Experiment Telescope (EGRET), the predecessor to *Fermi*, was responsible for the discovery of about five young pulsars. A binary millisecond pulsar, PSR J1816+4510, was first detected by *Fermi* as a gamma-ray source. The pulsar was then found as a source of radio pulsations in the Green Bank North Celestial Cap (GBNCC) survey using the coordinates of the unclassified *Fermi* source 2FGL J1816.5+4511 [3]. From extensive radio observations of PSR J1816+4510, it was found to be a binary millisecond pulsar with many interesting parameters (See [4]).

Figure 1 shows the gamma-ray detection of PSR J1816+4510 in `PRESTO` plot format. The upper left corner image of the figure is the pulse profile of the pulsar's gamma-ray emission. The y-axis represents power. The plot is a visual representation of the pulsar's gamma-ray pulsations showing the amplitude of the emission at the time in its rotation where this emission occurs. It looks much like a radio pulsar's profile. The plot on the lower left, below the pulse profile, is the persistence plot. It shows if the pulsar's signal is showing up throughout the entire observation time. The remaining plot is the trial period-period derivative plot showing the optimal period versus period derivative. The x-axis for these plots is in the phase representation of time.

According to Lorimer and Kramer [5], "a new definition of pulsar should perhaps be a neutron star that emits radiation that is pulsed due to rotation and powered by rotational energy." This is in reference to pulsars not being confined to the classical model of radio-wave emitting neutron stars, but also ultra-violet, X-ray and gamma-ray emitting as well. Based on the populations of pulsars found across a great range of energies and those with emission in multiple spectra, the astronomy community must adapt previous notions of what a pulsar is.

Our goal is to discover gamma-ray pulsations from newly discovered radio pulsars. This detection is possible, given that many gamma-ray pulsars have

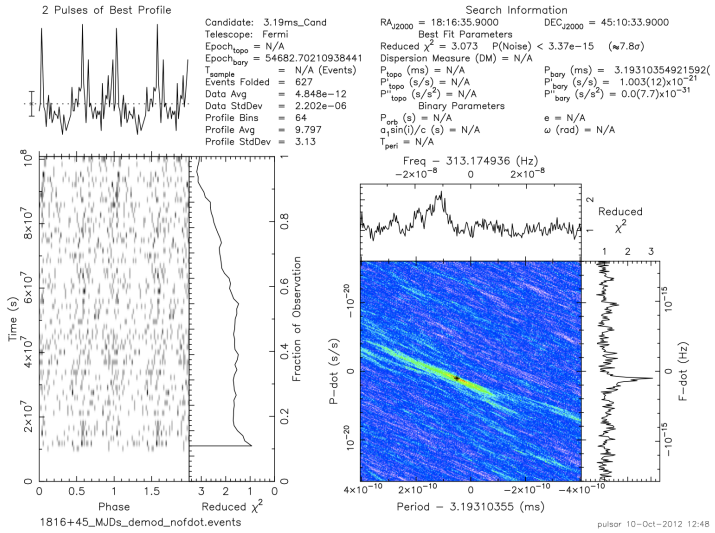

Figure 1: Gamma-ray pulsations of PSR J1816+4510 in `PRESTO` plot format. It includes the periodic gamma-ray emission profile in the upper left-hand corner. Below that is the phase versus time representation of its period, or persistence plot. The plot in the lower right-hand corner is the optimal period-period derivative plot. The approximate period is 3.19 ms and the number of events is 627.

been discovered from unclassified gamma-ray sources from the LAT survey. It would be useful to find a pattern among radio pulsars which tend to pulse in gamma-rays and those that do not. The interesting parameters of J1816+4510 demonstrate the validity of the work to detect gamma-ray pulsations from other pulsars.

Besides J1816+4510, we have analyzed ten other pulsars for gamma-ray pulsations. No detection was made on these other pulsars. This is not indicative of a lack of gamma-ray pulsation from these pulsars. Rather, there are several factors which limit our ability to detect gamma-ray pulsations from these pulsars. The events that were taken into account were specifically greater than 300 MeV and within a search radius of 0.92 degrees—the values used for the initial analysis for J1816+4510. Thus the next step will be to change or expand the parameters used in the search for gamma-ray pulsations. Also, improved ephemerides for some of these pulsars may lead to some detections. It is possible to make detections for several of these pulsars. Once we find the best radius and minimum energies to use we will

improve the likelihood of detection. Figure 2 shows the photon counts as a function of phase for gamma-ray data in the direction of PSR J0636+51. This is a result of the initial folding and cuts of an energy minimum of 300 MeV and a radius of 0.92 degrees.

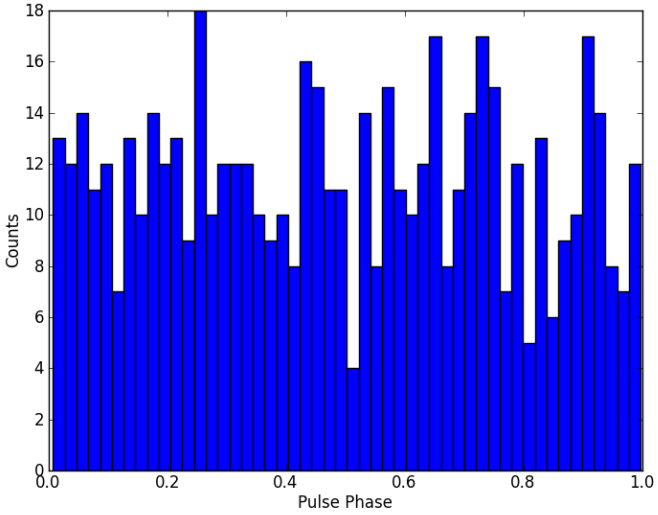

Figure 2: Counts versus pulse phase for gamma-ray data obtained for PSR J0636+51 using a cutoff energy of 300 MeV and a cutoff radius of 0.92 degrees.

The pulsars that are being analyzed represent a spectrum of pulsars. They are combinations of millisecond, binary, young, recycled, and normal pulsars, which makes for a good survey of pulsar types from which to detect gamma-rays. The pulsars we evaluated are J0636+51, J0645+51, J0931-19, J1432+72, J1907+06, J1911+22, J1957+25, J1950+24, J1933+17, and J1910+05. Of these pulsars, two are normal pulsars (J1911+22 and J1910+05), one is a young pulsar (J1907+06), one is an isolated partially recycled pulsar (J1432+72), two are isolated MSPs (J0645+51 and J0931-19), and four are binary millisecond pulsars (J0636+45, J1957+25, J1950+24, and J1933+17, which is also partially recycled).

The outline of this paper is as follows. Section 2 describes the motivation behind the work done in this paper. The section which details the *Fermi* LAT is Section 3. Section 4 contains background on the H-test and testing

for periodicity in the data. In Section 5 we discuss the methods used to analyze the pulsars for gamma-ray pulsations. The results, including parameters of the pulsars being analyzed, are contained in Section 6. Folded gamma-ray plots for pulsars J1816+4510 and J0636+51 are also in this section. A discussion of the results and future work is in Section 7. Section 9 provides folded gamma-ray plots for the remaining nine pulsars.

2 Motivation

According to P.S. Ray et al., known pulsars are a "prevalent class" of GeV gamma-ray sources [2]. Therefore searching known radio pulsars for pulsed gamma-ray emission is justified. Detection of unique properties of these pulsars may be feasible through gamma-ray pulsation detection. In the case of J1816+4510, many such UV/optical properties have been found [4]. If a detection cannot be made, it will be of key importance to determine why a detection cannot be made and to determine whether or not this means there is no periodic gamma-ray emission from the pulsar or whether there is some other explanation.

The *Fermi* Pulsar Search Consortium (PSC) is an international collaboration of radio astronomers and members of the LAT collaboration. Their goal is to organize radio follow-up observations of pulsars found in *Fermi* and pulsar candidates from among the LAT gamma-ray sources. From the 35 LAT-discovered pulsars found in the PSC's blind frequency searches, radio pulsations were detected from four, through extremely in-depth radio observations of all of them [2]. The characteristics of these four pulsars are worth looking at since they are periodic both in radio and gamma radiation. Using J1816+4510 as our model pulsar, we would like to research other radio pulsars to see if we can detect gamma-ray pulsations from them.

When gamma-ray emission is detected, it means that a major event has happened to give off this high energy. The observation of very high energy systems is possible through this area of research. While there is a huge effort by the PSC to find pulsars from the LAT survey, there is not as much involvement in the reverse search of pulsed gamma-ray emission from radio pulsars. It is important to look at the most likely candidates for success in this search. These are millisecond pulsars and young pulsars; however, it is possible that all types of pulsars pulse in gamma radiation. Therefore we will not limit our analysis to only millisecond and young pulsars.

3 *Fermi* LAT

The LAT is an imaging high-energy gamma-ray telescope covering the energy range from about 20 MeV to more than 300 GeV. The LAT's field of view at any moment is 20 percent of the sky. It scans continuously and covers the entire sky every three hours. The angular resolution of LAT depends on the gamma-ray's energy. For 100 MeV the angular resolution for a single photon is less than 3.5 degrees [6]. Data from LAT is available to the public along with standard analysis software at the Fermi Science Center.

Gamma-ray detectors are completely different from radio and optical telescopes because gamma-rays cannot be focused like ordinary light [7]. They also cannot be refracted by a lens like visible light. It is not surprising, then, that there are challenges present with gamma-ray detectors. The casing surrounding the telescope can be infiltrated by gamma-rays resulting in a haze and obscuring the object being studied. Free electrons hitting the detector can also mimic a gamma ray signal, and thus represent a noise source. That is not to say that gamma-rays are not hitting the detector as well, but the noise coming from cosmic rays can drown out the signal. The LAT must be able to distinguish this background noise from the desired signal, if any.

Detection of gamma-ray pulsations can be made by using the H-test as the statistical test by which we measure the probability that a periodic signal is present. Periodicity of the data is what we are referring to when we talk about gamma-ray pulsations. If we do detect these pulsations, we want to characterize the pulsar's gamma-ray emission. If we do not detect gamma-ray pulsations, we want to place an upper limit on the gamma-ray emission, explore the possible reasons why gamma-ray emission was not detected, and what we could do to improve the likelihood of making a detection.

4 The H-test

In order to test for periodicity in a data set, we need to use a statistical test. We use the H-test because it is the best-all around test for periodicity when the shape of the light curve is unknown [8]. The H-test is defined in terms of the Z_m^2 statistic, which we describe first.

Consider a set of arrival times t_i with $(i = 1, 2, 3, ..., n)$, where n is the total number of data points, and phases θ_i on the interval $[0, 2\pi)$, obtained by folding the arrival times with respect to some period. To test for uniformity (i.e., flatness) in the light curve we consider the null hypothesis. The

null hypothesis represents the absence of a signal. The mathematical representation of this hypothesis is a constant (uniform) light curve, which makes sense since there would be no significant variation in the data in the absence of a periodic signal. Let $f(\theta)$ be the unknown light curve of the folded arrival times (i.e., events). Then the null hypothesis, H_0, is defined as $f(\theta) = 1/2\pi$ with θ running from 0 to 2π. Under the alternative hypothesis, H_A, we have

$$f(\theta) = pf_s(\theta) + (1-p)/2\pi, \tag{1}$$

where $f_s(\theta)$ is the light curve for a possible signal and p is a number between 0 and 1. One can see that for $p = 0$, $f(\theta) = 1/2\pi$, which corresponds to the absence of a signal (i.e., null hypothesis). For $p = 1$, $f(\theta) = f_s(\theta)$, which corresponds to a pure signal. To determine whether a periodic signal is present, we must decide whether to accept or reject the null hypothesis.

Therefore we define a functional $\psi(f)$ that represents the distance between $f(\theta)$ and its value, $1/2\pi$, in the absence of a signal:

$$\psi(f) = \int_0^{2\pi} (f(\theta) - 1/2\pi)^2 d\theta. \tag{2}$$

Since $f(\theta)$ is not known, we need to estimate it from the data. Following [8], we define a Fourier series estimator of $f(\theta)$ having m harmonics:

$$\hat{f}_m(\theta) = \frac{1}{2\pi}[1 + 2\sum_{k=1}^{m}(\hat{\alpha}_k \cos k\theta + \hat{\beta}_k \sin k\theta)], \tag{3}$$

where the Fourier coefficients are calculated from the data θ_i using

$$\hat{\alpha}_k = (1/n)\sum_{i=1}^{n} \cos k\theta_i \;\text{ and }\; \hat{\beta}_k = (1/n)\sum_{i=1}^{n} \sin k\theta_i\,. \tag{4}$$

Plots of $\hat{f}_m(\theta)$ show that they are approximations to a histogram of the phases θ_i. Lower values of m correspond to smoother (i.e., coarser) approximations to the histogram, while for larger values of m, $\hat{f}_m(\theta)$ more closely follows bumps in the histogram (Joe Romano, private communication). The Z_m^2 statistic is then defined as

$$Z_m^2 = 2\pi n \psi(\hat{f}_m) = 2n\sum_{k=1}^{m}(\hat{\alpha}_k^2 + \hat{\beta}_k^2), \tag{5}$$

where the second equality follows from the previous definitions and the orthogonality of sines and cosines. The Z_m^2 statistic is basically the power in the first m harmonics of a Fourier series estimator of the light curve $f(\theta)$.

Once we have the Z_m^2 statistic, the H statistic is easily calculated. It is defined as:

$$H = \max_{1 \leq m \leq 20} (Z_m^2 - 4m + 4) = Z_M^2 - 4M + 4, \tag{6}$$

where M is the value of m that maximizes the function $Z_m^2 - 4m + 4$. As mentioned in [8], M is also the value of m that gives the best Fourier series estimator $\hat{f}_m(\theta)$ of the true light curve $f(\theta)$ in the sense that it minimizes the *mean integrated squared-error* (MISE) between the estimator and the true light curve:

$$\text{MISE}(m) = \int_0^{2\pi} (\hat{f}_m(\theta) - f(\theta))^2 d\theta. \tag{7}$$

Thus M tells us the optimal number of harmonics to use.

Since H is basically Z_M^2, and Z_M^2 is proportional to the squared distance of the estimator $\hat{f}_m(\theta)$ away from a flat light curve, a large value of H corresponds to a low probability that the measured periodicity is caused by noise alone (i.e., that it is a false alarm). Thus, the value of the H statistic and the false alarm probability are inversely related to one another (the higher the value of the H statistic, the lower the false alarm probability will be and vice versa). The false alarm probability must be very close to zero if we are to reject the null hypothesis and say that we have detected a periodic signal. As shown in de Jager and Büshing [9], the probability distribution for the H-test statistic in the absence of a signal is given by

$$P(H > h) = e^{-0.4h} \tag{8}$$

This formula tells us the probability that H is greater than some threshold value h, if the null hypothesis is satisfied. For example, if we measure $H > 23$, we can reject the null hypothesis with a false probability of less than $e^{-0.4 \times 23} \approx 1 \times 10^{-4}$ and claim a significant detection. For values of $H < 23$, the false alarm probability will be higher, and we would not reject the null hypothesis for these cases.

5 Methods

In order to download photon data for a pulsar, LAT data is obtained using the coordinates of the pulsar (right ascension (RA) and declination (DEC)). Folding is the addition of many pulses so that the signal is visible above the background noise. It works the same for both gamma-ray pulses and

for radio pulses. Our analysis involves folding gamma-ray data obtained from the LAT data server, and performing selection steps on the data which limit the energy range and radius around the coordinates that are taken into account. Since gamma-rays are the highest energy electromagnetic waves, it is more likely that the lower energy photon data could include noise. Therefore the data obtained from LAT must be optimized by limiting the lower energy photons that we include in our analysis. Once the LAT data is obtained, basic cuts to the data are made, and then the data is folded based on a minimum energy (i.e. , cutoff energy) and radius (i.e. , cutoff radius).

The first step to making a detection for radio pulsars which are not known to pulse in gamma-rays is to be sure that a detection can be made with a known gamma-ray and radio pulsar. PSR J1816+4510 is one such pulsar on which the analysis can be performed. The ephemeris consists of important parameters of the pulsar such as its right ascension and declination, the period, period derivative and orbital parameters if applicable—additional parameters that describe the orbit of a binary pulsar and its companion, such as orbital period. Using J1816+4510's radio ephemerides, pulsations were detected by Kaplan et al. from the unclassified gamma-ray source 2FGL J1816.5+4511, adding pulsar J1816+4510 to the many millisecond gamma-ray pulsars detected by *Fermi* [4]. The position is given by a right ascension of 18:16:35.9314(2) and a declination of 45:10:33.864(2). We will also use the pulsars' ephemeris in our analysis.

The detection made by Kaplan et al. of significant gamma-ray pulsations from PSR J1816+4510 was obtained using an analysis which includes the use of Fermi science tools [4]. Replication of this detection will confirm our ability to detect gamma-ray pulsations when they are present. After reasonable replication of the results, the analysis can be applied to other radio pulsars in hopes of making first-time gamma-ray pulsation detections for these pulsars. In this paper we shall evaluate 10 radio pulsars besides J1816+4510 for gamma-ray pulsations.

The photon data must be obtained from the online LAT data server. This can be found at `http://fermi.gsfc.nasa.gov/cgi-bin/ssc/LAT/LATDataQuery.cgi`. The specific photon data that we are looking for is in the energy range of gamma radiation. In the electromagnetic spectrum, gamma radiation is greater than 100 keV. This corresponds to frequencies greater than 10^{19} Hz, which encompasses wavelengths of less than ten picometers.

Standard procedures for data preparation can be found at `http://fermi.gsfc.nasa.gov/ssc/data/analysis/scitools/data_preparation.html`. The software and tools needed for our analysis consist of `PRESTO`,

`tempo2`, `python`, and the Fermi Science Tools. Before analyzing the radio pulsars from which we want to find gamma-ray pulsations, it was necessary to confirm that gamma-ray pulsations could be detected from a known gamma-ray and radio pulsar. PSR J1816+4510 was thus the first pulsar to be analyzed since it is both a gamma-ray and radio pulsar. The results and a plot of the folded gamma-ray data for J1816+4510 are included in Section 6.

We obtained ephemerides for ten pulsars (Stovall, private communication). The RA and DEC for each pulsar were completely converted into degrees in order to download the LAT data for these pulsars. The Modified Julian date (MJD) is a standard astronomical time unit which we use to specify the time range of data to obtain. In the LAT data server query parameters, the time range is set from the date of *Fermi's* 1st mission (MJD 54682.655) up to the date the files are downloaded, so that all the data available can be retrieved. The actual time span of data used in the folding will be different from the ones used to retrieve photon data. For practical purposes it is best to retrieve all the photon data for each pulsar and then use the same time span which best suits our needs for all pulsars when folding the data. In order to compare the pulsars, it is best to analyze the photon data from within the same time range. We use the default energy range, a minimum of 100 MeV and maximum of 300000 MeV (300 GeV). A search radius must also be specified unless using the default value of 15 degrees. All these parameters must be specified in order to obtain all of the available data. Eventually the parameters that go into the actual processing of the data will be changed. All of the files which the search provides are downloaded. The files are events and spacecraft files in the FITs format. The FITs format is a standard digital file format that is commonly used in astronomy. The spacecraft data is information about the location and orientation of the spacecraft at 30 second intervals. Regardless of the size of the data set, there will be only one spacecraft file [10].

Processing of data was done using the Fermi Science tools which can be found at `http://fermi.gsfc.nasa.gov/ssc/data/analysis/software/`. The first step to data processing is using a tool called gtselect. Gtselect will make cuts to the events data files. It creates a filtered FITs file based on user-specified cuts to the infile which is the event data file. The cuts are typically made to bound the dataset's time range, energy range, region of interest radius, and maximum zenith angle [11]. Then gtmktime creates good time intervals (GTIs), which are time ranges where data can be considered valid, based on selections made using spacecraft parameters [12]. The selection of time ranges when the data quality is good will eliminate times when

some spacecraft event has affected the quality of the data [13]. This cut is necessary to ensure that we use the optimal data in our analysis. We must specify the data quality we want to use in the gtmktime command. We chose DATA_QUAL= 1. Other integer values are not good for our analysis such as 0, which is bad data that should not be used, and -1, which is a time when the data was affected by a solar flare [14]. Neither of these are data types that we should use.

The phase is a particular stage in a periodic process. In this case it is a particular stage in the rotation of the pulsar. The Fermi plugin for `Tempo2` assigns phases to all of the events. Finally a `python` script called `fermi.py` is used to process the data, applying a minimum energy and radius cut. The script `fermi.py` also specifies the time range in which we want the data to be folded. For the gamma-ray data the folding is done using the period of the pulsar specified by its radio ephemeris.

For multiple minimum energy and radius cuts, we run a `python` script that utilizes a loop that will pass these arguments to `fermi.py` and output these values along with the H statistic into a file that we can look at and see where we get the largest value of the H statistic. Figures 2- 13 were produced by folding the data from MJD 54682.698 to 55943.984 for PSRs J1816+4510, J0636+51, J0645+51, J1907+06, J0931-19, J1911+22 and from MJD 54682.655 to 56035 for PSRs J1432+72, J1957+25, J1950+24, J1933+17, J1910+05. The above script was written (with help from Kevin Stovall and Alex Garcia) in order to pass several energy and radius cuts to `fermi.py`. Initially we only passed one value for the cutoff energy and cutoff radius.

The goal of passing several values is to see how the H statistic changes as these values change. We can expect the H statistic to change when more or less noise affects the signal. An explanation of how more or less noise can be filtered is found in the Conclusions section. The reason for testing for periodicity for many minimum energies is because we do not know what the minimum energy of the pulsations from the pulsar would be if it was pulsing in gamma-rays. Neither do we know the size of the area from which the signal is coming, and this is why we test for periodicity for different radii. If our energy cutoff value is too low then we may be including noise, and if it is too high we could be leaving out some of the signal. The basis for using several radii is analogous to why we use several energies: too big of a radius will include too much noise and too small of a radius would cut out some of the signal.

The resulting H statistic values can be plotted against the minimum energy and radius and evaluated to see what would be a good range of

values to use for further analysis. We did this for J1816+4510. Our analysis showed that there was a distribution around the cutoff radius which would be desirable to evaluate, while the energy seemed to not give a good indication of what range to use. We also look at the folded gamma-ray data in order to see the pulsations or lack thereof. This is represented by the plot of counts vs. pulse phase like shown in Figure 3. The phase corresponds to a fraction of the pulsar's cycle. The x-axis goes from 0 to 1, which corresponds to phase angles between 0 and 2π.

This analysis was first performed on PSR J1816+4510. The gamma-ray pulsation detection that Kaplan et al. obtained was confirmed in order to verify that a detection could be made. The H-test statistic that resulted was about 110.56 [4].

When pulsations are not detected we must place a limit to the emission which can be detected for these pulsars. This is given by the count rate. The count rate is calculated by dividing the number of photon counts detected by the time in which these counts were detected. This means that we must find the amount of time the LAT detector was actually pointing at and collecting data from the source or pulsar, which will be different from the time over which we are folding the data. In mathematical notation, where C is the count rate, c is the number of photon counts, and t is the amount of time in which the counts were collected, $C = c/t$.

6 Results

Using the analysis software and tools, we were able to confirm the detection of gamma-ray pulsations from PSR J1816+4510. In analyzing the ten other pulsars, no periodic gamma-ray emission was detected. The results can be seen from the counts versus pulse phase plots (see Figs. 4- 13) and the H-statistic values and probabilities in Table 1, which were obtained from the `fermi.py` python script. The H-statistic value gives an indication of whether or not periodic gamma-ray emission was detected. It results from a set of input values, the cutoff energy and cutoff radius.

For J1816+4510 we not only confirmed periodicity using the same cutoff energy and radius as Kaplan et. al, but we also folded the photon data at multiple energy and radius cutoffs. One very important result was improving the H statistic by using a range of energy and radius cuts. For the initial values used as cuts for J1816+4510, the result was an H statistic value of 110.56. Using a range of energy and radius cuts, the largest H statistic value of 111.82 was obtained with a minimum energy of 360 MeV and a

radius of 1.0 degrees. This shows that we can optimize the energy and radius cuts to improve our results, yet only marginally. To evaluate whether or not this is a significant increase in the H statistic, it is probably best to look at the corresponding decrease in probability this results in. This only makes a difference of $6.17\text{x}10^{-11}$ in the probability, on the order of one magnitude less than the probabilities themselves. The values obtained for the H statistic are fairly close to the value obtained by Kaplan et al. [4]. The folded gamma-ray data of J1816+4510 for cutoff energy and radius of 360 MeV and 1.0 degree, respectively, is shown in Figure 3. To learn more about J1816+4510's properties, including gamma-ray and UV/optical, see [4].

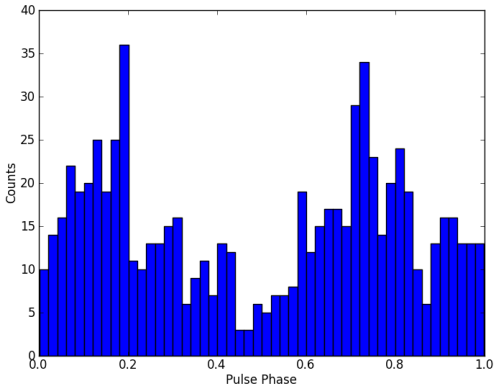

Figure 3: Counts versus pulse phase for J1816+4510 with energy and radius cutoffs which optimize the H-statistic value. The cutoff energy is 360 MeV and the cutoff radius is 1.0 degree.

For a radius cutoff of 0.92 degrees and energy cutoff of 300 MeV (the values for which periodicity of the gamma-ray emission was detected for PSR J1816+4510), the analysis yielded no finding of gamma-ray pulsations for all ten pulsars. For PSR J0636+51 analysis at many radii and energy cuts did not yield a detection of gamma-ray pulsations. The cutoff energies used for PSR J0636+51 ranged from 100 MeV to 490 MeV and the cutoff radii ranged from 0.1 to 4.9 degrees. For PSR J1957+25 we were able to perform the analysis using cutoff energies from 100 to 190 MeV and radius cuts from 0.1 to 4.9 degrees. For J0645+51 we were able to do so for combinations of 100 MeV for the energy cutoff and 0.1 to 1.1 degrees for the radius.

Figure 4 shows the counts versus pulse phase of PSR J0636+51 at an

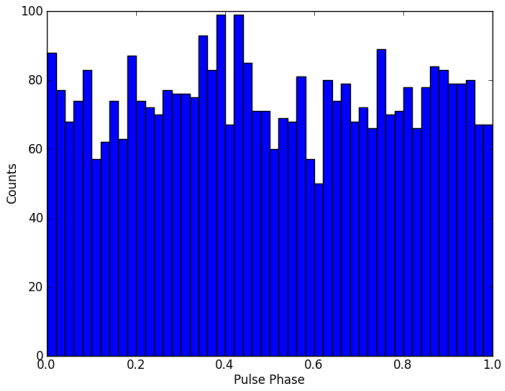

Figure 4: Counts versus pulse phase for J0636+51 with an energy cutoff of 290 MeV and a radius cutoff of 2.4 degrees.

energy cutoff of 290 MeV and a 2.4 degree radius. These are the cutoff values which yielded the highest H statistic value for J0636+51, which was found by combing through the output file which came from the script which passed several energy and radius cutoffs. The highest H statistic value obtained was 9.8 (false alarm probability of 0.02). It can be seen that there is no periodicity of gamma-rays coming from PSR J0636+51. The folded data is generally flat just like with the other nine pulsars. PSR J0636+51 has been timed for less than a year. Its timing solution is yet to be perfected. In the conclusion section we discuss more about the timing solution and its relevance to being able to detect gamma-ray pulsations. The minimum H statistic value we obtained for any of these pulsars was 0.02 and the highest was 9.8. These are insignificant H statistic values.

We were able to fold data at more radius and energy cutoffs for pulsars further from the galactic plane due to less background noise. The galactic plane contains massive amounts of photon data. For PSR J1907+06, there were simply too many events to evaluate it at more than just one minimum energy and radius cut. Because excessive photon data prevented several sets of values to be passed to `fermi.py`, we evaluated seven of the pulsars only at 300 MeV and 0.92 degrees. For PSR J1907+06, it resulted in an H statistic value of 1.32 (false alarm probability of 0.59). The counts versus pulse phase for J1907+06 with an energy cutoff of 300 MeV and 0.92 degrees is shown in Figure 8. Table 1 includes the period, the coordinates, the H statistic value,

and the probability for each pulsar. RA is in hours:minutes:seconds, and DEC is in degrees:arcminutes:arcseconds. An arcminute is 1/60 of a degree and an arcsecond is 1/60 of an arcminute. This table includes the improved H statistic obtained for PSR J1816+4510. The count rate is given in counts per year. The values in Table 1 are for data folded from MJD 54682.698 to 55943.984.

Pulsar	P	RA	DEC	H Statistic	Prob.	Count rate
J1816+4510	3.19	18:16:36	45:10:34	111.82	4.81e-20	—
J0636+51	2.86	06:36:05	51:28:60	0.34	0.87	360.17
J0645+51	8.85	06:45:59	51:58:15	6.14	0.086	295.41
J0931-19	4.64	09:31:19	-19:02:55	6.1	0.087	389.97
J1432+72	41.7	14:34:44	72:47:19	0.46	0.83	75.396
J1907+06	324	19:07:04	06:31:17	1.32	0.59	20635.95
J1911+22	320	19:11:13	22:33:08	0.02	0.99	1597.02
J1957+25	3.96	19:57:35	25:16:02	1.82	0.48	3674.7
J1950+24	4.30	19:50:45	24:14:57	4.72	0.15	4661.6
J1933+17	21.5	19:33:22	17:28:07	0.48	0.83	2005.8
J1910+05	308	19:10:39	05:17:38	2.06	0.44	2325.6

Table 1: The pulsars' partial ephemeris, H statistic, and count rate. P represents the period in milliseconds, RA is the right ascension, DEC is the declination, H statistic refers to the H statistic for each pulsar at a cutoff energy of 300 MeV and a cutoff radius of 0.92 degrees (except for J1816+4510 which had an optimized H statistic at a cutoff energy of 360 MeV and a cutoff radius of 1 degree). Probability is the false alarm probability (the chance of getting an H statistic value this large or larger when no signal is present). The count rate is the number of counts received over the total amount of good time intervals which were spent pointed at the pulsar. The count rate is given in counts per year.

In Table 1 "H statistic" refers to the H statistic values which were obtained using energies greater than 300 MeV and a radius of 0.92 degrees. "Probability" refers to the false alarm probability (i.e., the probability of getting an H-statistic value this large or larger in the absence of a signal). For J0645+51 the highest H statistic value of 9.04 was achieved for a cutoff energy of 100 MeV and radius of 0.5 degrees. Probabilities were computed using Equation 8. These H statistics values are not significant, which follows from their relatively large false alarm probabilities.

7 Conclusions

We analyzed the known gamma-ray pulsar J1816+4510, showing that we could detect gamma-ray pulsations. We then analyzed 10 newly discovered known radio pulsars, which resulted in non-detections for all ten. If

gamma-ray pulsations are not being detected, it does not mean they are not present in the data. We cannot simply conclude that the signal is flat because we have not found evidence that shows otherwise. There are two major hindrances which keep us from concluding that the ten pulsars are not gamma-ray pulsars: one is the lack of a good timing solution for most of the pulsars, and the second is not having had enough time to fold the pulsars for many ranges of energy and radii. The folding of the pulsar data for different cutoff energies and radii is computationally expensive.

It is important to have a good timing solution for a pulsar—like all of the radio pulsars which have been found to pulse in gamma-rays—in order to understand the pulsar's rotational characteristics. A timing solution is basically accurate information on the pulsar related to when a signal will arrive at the detector. To obtain a good timing solution (i.e., the period and period derivative are accurate and well known), the pulsar usually must be observed over the course of more than a year. Most of the pulsars evaluated in this paper have been timed for little over a year. On that basis, it is not surprising that the pulsars analyzed in this paper were not conclusive. If the timing solutions of these pulsars were accurate, then we could say that they are not pulsing in gamma-rays, but that is not the case.

In terms of pulsar timing, the period derivative and the position (RA and DEC) are covariant for the first year. After a year of timing, the period derivative and position start to be less covariant. The pulsars J0636+51, J0931-19, J1957+25, and J1933+17 have been timed for less than a year. The pulsars J1432+72, J1911+22, and J1910+05 have been timed for about a year. The pulsars J0645+51, J1907+06, and J1950+24 have been timed for more than a year. There is a limit to the detectable amount of counts for any given year or period of time for each of these pulsars. Pulsars which have higher counts due to them being located near the galactic plane will have higher limits. This means that limits for some pulsars will be more significant than for other pulsars.

Being able to optimize the cuts with many energy and radius cutoffs for each pulsar will allow for data to be processed which maximizes the chances of making a detection. There is a big range of energies that gamma-rays encompass and many radii which would allow for a suitable area to be examined that maximizes the gamma-rays which come from the actual source of interest. In light of this, it is necessary to explore many ranges for folding the data in order to properly evaluate the pulsar's gamma-ray emission. As mentioned earlier, gamma-rays cannot be focused like ordinary light, therefore a cutoff radius of 1 degree does not make as big a difference here as it does when searching for radio pulsars. We can also obtain a higher

H statistic value by expanding the time range in which we fold the data.

We also need to minimize the radius, or maybe this kind of analysis should be reserved for pulsars which are not right in the galactic plane. For pulsars located in this region it is possible that even if gamma-ray periodicity was present, the signal would not be distinguishable due to all the bombardment of noise from the surrounding region. Processing of data for these pulsars definitely takes more time, which is something that should be taken into consideration.

Thus future work will include folding the pulsar gamma-ray data when a better timing solution is derived for these pulsars. If we have a good timing solution and are still not able to detect pulsations, then we have better reason to conclude that the pulsars are not gamma-ray pulsars. We also would like to continue evaluating all the non-conclusive pulsars with several radius and energy cutoffs. In this way we can determine for what radius and energy cutoff we get a higher H statistic and how the H statistic increases and decreases around that value. Once the data is folded with good timing solutions and a range of energy and radius cutoffs, we can determine a better limit. Once we can confirm which of these radio pulsars are gamma-ray pulsars, it would be of interest to find which properties and characteristics the gamma-ray pulsars share.

Other future work includes calculations of the flux limits for these pulsars. Using the size of the collecting area and the count rate for each pulsar, along with the energy for each photon, we can calculate these limits. These limits are calculated when the analysis does not yield a detection.

8 Acknowledgments

I would like to thank my mentor Kevin Stovall and my advisor Dr. Frederick Jenet. I would also like to thank graduate student Alex Garcia for teaching me how to write python scripts. Thank you Dr. Joseph Romano and Dr. Matthew Benacquista for all the comments and help in the revision process. Thank you to the entire ARCC committee. I would like to dedicate this thesis to my late father, Lawrence Cohen, who has motivated and inspired me to be a scientist and an engineer. I would also like to acknowledge my mother who has always been supportive of me. I would like to thank the National Science Foundation (NSF) for the grants which support this research, AST0545837 and AST0750913.

9 Appendix

This section contains the rest of the counts versus pulse phase plots for the pulsars evaluated in this paper. Section 6 contains the counts versus pulse phase plots for PSR J1816+4510 and J0636+51.

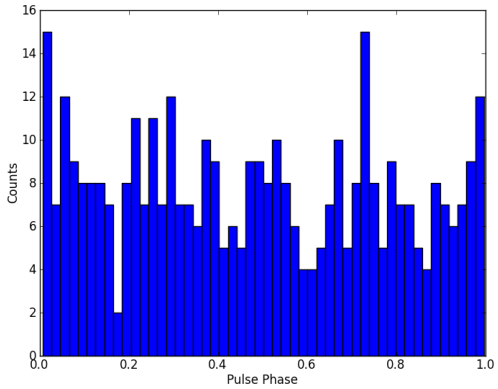

Figure 5: Counts versus pulse phase for J0645+51 with an energy cutoff of 300 MeV and a radius cutoff of 0.92 degrees.

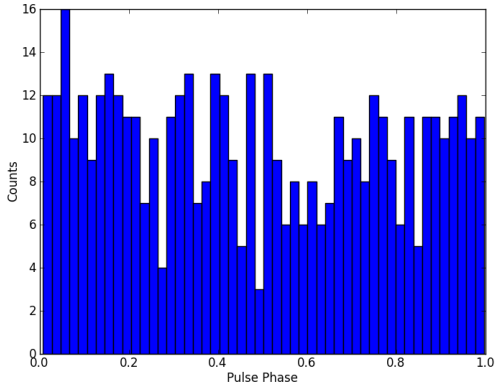

Figure 6: Counts versus pulse phase for J0931-19 with an energy cutoff of 300 MeV and a radius cutoff of 0.92 degrees.

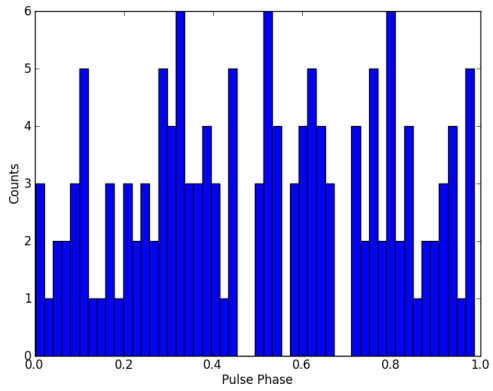

Figure 7: Counts versus pulse phase for J1432+72 with an energy cutoff of 300 MeV and a radius cutoff of 0.92 degrees.

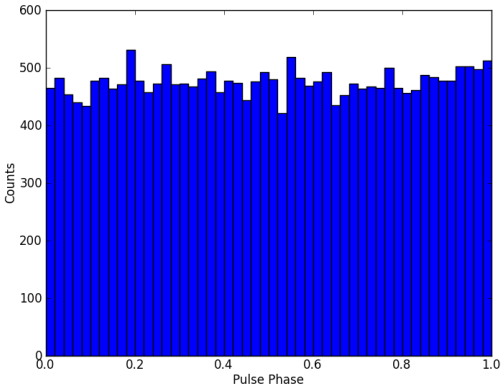

Figure 8: Counts versus pulse phase for J1907+06 with an energy cutoff of 300 MeV and a radius cutoff of 0.92 degrees.

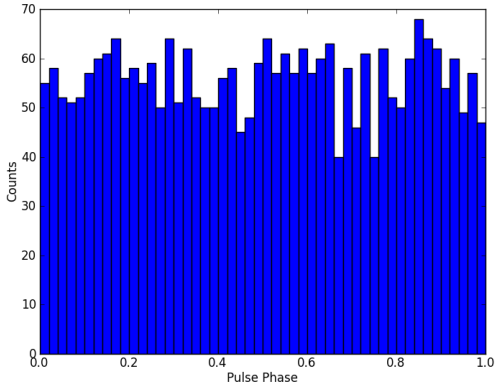

Figure 9: Counts versus pulse phase for J1911+22 with an energy cutoff of 300 MeV and a radius cutoff of 0.92 degrees.

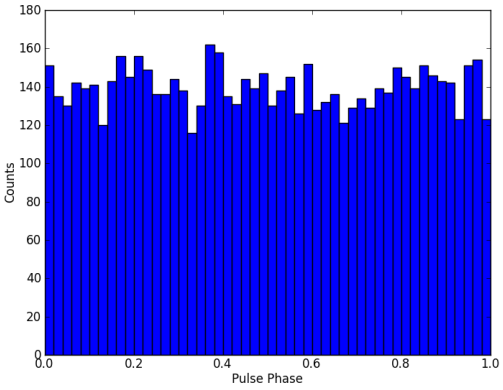

Figure 10: Counts versus pulse phase for J1957+25 with an energy cutoff of 300 MeV and a radius cutoff of 0.92 degrees.

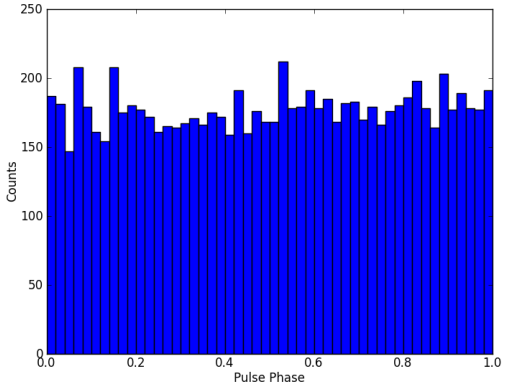

Figure 11: Counts versus pulse phase for J1950+24 with an energy cutoff of 300 MeV and a radius cutoff of 0.92 degrees.

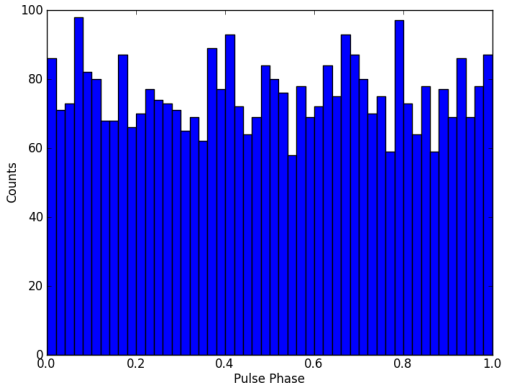

Figure 12: Counts versus pulse phase for J1933+17 with an energy cutoff of 300 MeV and a radius cutoff of 0.92 degrees.

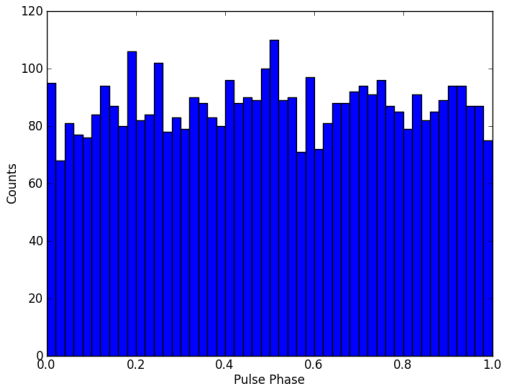

Figure 13: Counts versus pulse phase for J1910+05 with an energy cutoff of 300 MeV and a radius cutoff of 0.92 degrees.

References

[1] `http://fermi.gsfc.nasa.gov/science/` (NASA *Fermi overview*, 2012).

[2] P. S. Ray *et al.*, "Radio Searches of Fermi LAT Sources and Blind Search Pulsars: The Fermi Pulsar Search Consortium," ArXiv e-prints (2012).

[3] Stovall *et al.*, in preparation (2013).

[4] D. L. Kaplan *et al.*, Astrophysical Journal **753**, 174 (2012).

[5] D. R. Lorimer and M. Kramer, in *Handbook of Pulsar Astronomy, 1st ed.*, (Cambridge University Press, Cambridge, U.K., 2005).

[6] `http://fermi.gsfc.nasa.gov/science/instruments/table1-1.html`.

[7] G. McNamara, in *Clocks in the Sky*, (Praxis Publishing, Chichester U.K., 2008).

[8] O. C. de Jager, B. C. Raubenheimer, & J. W. H. Swanepoel, Astronomy and Astrophysics **221**, 180 (1989).

[9] O. C. de Jager, I. Büshing, Astronomy and Astrophysics **517**, L9 (2010).

[10] http://fermi.gsfc.nasa.gov/ssc/data/analysis/scitools/extract_latdata.html.

[11] http://fermi.gsfc.nasa.gov/ssc/data/analysis/scitools/help/gtselect.txt.

[12] http://fermi.gsfc.nasa.gov/ssc/data/analysis/scitools/help/gtmktime.txt.

[13] http://fermi.gsfc.nasa.gov/ssc/data/analysis/documentation/Cicerone/Cicerone_Data_Exploration/Data_preparation.html.

[14] http://fermi.gsfc.nasa.gov/ssc/data/analysis/documentation/Cicerone/Cicerone_Data/LAT_Data_Columns.html.